A feedback control scheme for reversing a truck and trailer vehicle

Claudio Altafini, Alberto Speranzon and Bo Wahlberg

Abstract— **A control scheme is proposed for stabilization of backward driving along simple paths for a miniaturized vehicle composed of a truck and a two-axle trailer. The paths chosen are straight lines and arcs of circles. When reversing, the truck and trailer under exam can be modeled as an unstable nonlinear system with state and input saturations. The simplified goal of stabilizing along a trajectory (instead of a point) allows to consider a system with controllable linearization. Still, the combination of instability and saturations makes the task impossible with a single controller. In fact, the system cannot be driven backward from all initial states because of the jack-knife effects between the parts of the multibody vehicle, sometimes it is necessary to drive forward to enter in a specific region of attraction. This leads to the use of hybrid controllers. The scheme has been implemented and successfully used to reverse the radio-controlled vehicle.**

Keywords— **Multibody wheeled vehicle, backward driving, jack knife, state and input saturation, hybrid automata.**

I. Introduction

This paper describes a feedback control scheme used to stabilize the backward motion of the radio-controlled truck and trailer shown in Figure 1. The miniaturized vehicle is a

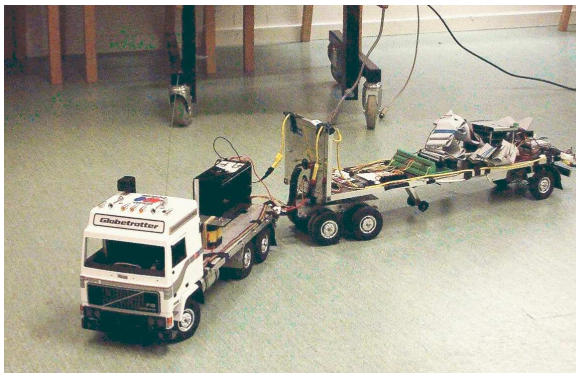

Fig. 1. The radio-controlled truck and trailer

(1:16) scale of a real commercial vehicle and reproduces in detail the geometry of the full-scale one; it has four axles, actuated front steering and actuated second axle to govern the longitudinal motion. Like the real one, it presents saturations on the steering angle and on the two relative angles between the bodies. It is equipped with potentiometers and differential encoders so that full state feedback is possible. Our control task is to drive the system backward along a preassigned straight line, avoiding jack-knive effects on the angles.

C. Altafini (corresponding author) is with the Division of Optimization and Systems Theory, Royal Institute of Technology SE-10044, Stockholm, Sweden; e-mail: altafini@math.kth.se

A. Speranzon and B. Wahlberg are with the Department of Signals, Sensors and Systems, Royal Institute of Technology, SE-10044 Stockholm, Sweden

There is a moderate literature on backward steering control of wheeled multiple vehicles reporting on experimental results achieved with different control techniques and with different kinds of vehicles, mainly expecially built laboratory mobile robots, see for example [15], [18], [20], [23], [30]. Numerous papers treat the backing problem with tools spanning from neural network [25], fuzzy control [11], [16], [30], learning, genetic algorithms and expert systems [6], [12], [17], [26]. Only a few works make use of more theoretical tools steaming from the literature on control of kinematic vehicles (overviewed for example in [5], [19]), see [7], [18], [29]. According to such formalism, our system is a general 3-trailer, general because of the kingpin hitching between the second axle and the dolly. The off-axle connection is important here because it indicates that the system is not differentially flat [9] neither feedback linearizable, and so simple motion planning techniques, like those based on algebraic tools [24] cannot be applied. See also [29] for reverse control of a truck with trailer via feedback linearization in the simpler case of no off-axle hitching.

From a system theory point of view, the control problem is quite challenging: it is an unstable nonlinear system with state and input constraints. The "reduced" control goal of stabilization along a line (instead of a point) allows to consider a system with controllable linearization, so that local asymptotic stability can be achieved via Jacobian linearization. Still, the combination of instability and saturations results in so-called jack-knife effects on the two relative angles between the truck and the dolly and between the dolly and the semitrailer. This makes the task of backward driving impossible to solve with a single controller. The scheme we use here is based on the observation that the system of equations is homogeneous in one of the inputs (the longitudinal velocity v). Homogeneity here means that the sign of v alone discriminates between forward and backward motion. The former, unlike reversing, is open loop stable, which implies that we can use it in order to get close enough to the equilibrium before switching to backward motion. The scheme is formalized in a switching controller with a logic variable that allows switching between the two different modes (forward and backward), each of them governed by a linear state feedback designed via linear quadratic techniques on the Jacobian linearizations. Switching in the logic variable occurs when the integral curve of the closed loop system hits suitably defined switching surfaces. There is a certain freedom in the design of the two switching surfaces, the important condition is that they do not touch each other. The criterion we follow here is that the reversing mode can be activated only when the system is entered inside the region of attraction of the local stabilizing controller. Since the nonlinear system is subject to saturations, very little can be said analytically about the region of convergence of a controller. However, an ellipsoid playing the role of invariant set for the closed loop saturated system can be identified by numerical methods. The second switching surface is meant to "inform" the controller that backward motion is going unstable and that a reallignement of the relative angles is needed (ac-

complished by moving forward). In the nominal system this second switching surface is never in use; however it is sometimes usefull in practice in order to reject disturbances and sensor errors. Furthermore, since the equilibrium occurs along a trajectory instead of a rest point, the (possibly destabilizing) perturbations affecting the system have to be considered as nonvanishing. In synthesis, the switching can be seen as an extra feedback loop around the two different closed loop modes. The switching surfaces and the switching logic are designed in such a way that the desired equilibrium inside the backward motion regime is given the character of global attractor from all the initial conditions in a prespecified domain. This switching scheme is described in Section IV. Once the local controllers for the different regimes of motion are available (linear feedback design in presence of saturation for forward/backward motion along lines/arcs is treated in Section III), there is a certain freedom in designing the logic loop. The choice above corresponds to the most elementary case of hybrid automaton (two states, two trasition rules) for the logic loop. As an example, in Section V we describe another simple enough scheme based on combinations of three different finite states. Both logic designs were implemented and successfully used to reverse the real vehicle. A few experimental tests are described in Section VI.

II. Kinematic equations and linearization

A. Kinematic model

Call $(x_3,\, y_3)$ the cartesian coordinates of the midpoint of the rearmost axle, θ_3 its absolute orientation angle, β_3 and β_2 the relative orientation angles respectively between the rearmost trailer body and the dolly and between the dolly and the truck body. L_3, L_2, M_1, L_1 are the lengths of the different parts of the body as indicated in Figure 2. The inputs are the steering angle α and the longitudinal velocity at the second axle v. The differential equations describing the kinematics are:

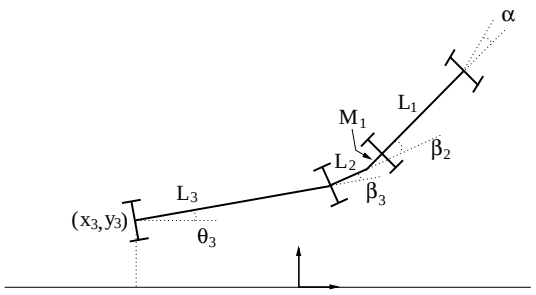

Fig. 2. The kinematic model of the truck and trailer

$$\dot{x}_3 = v\cos\beta_3\cos\beta_2\left(1+\frac{M_1}{L_1}\tan\beta_2\tan\alpha\right)\cos\theta_3 \quad (1)$$

$$\dot{y}_3 = v\cos\beta_3\cos\beta_2\left(1+\frac{M_1}{L_1}\tan\beta_2\tan\alpha\right)\sin\theta_3 \quad (2)$$

$$\dot{\theta}_3 = v\frac{\sin\beta_3\cos\beta_2}{L_3}\left(1+\frac{M_1}{L_1}\tan\beta_2\tan\alpha\right) \quad (3)$$

$$\dot{\beta}_3 = v\cos\beta_2\left(\frac{1}{L_2}\left(\tan\beta_2-\frac{M_1}{L_1}\tan\alpha\right)-\frac{\sin\beta_3}{L_3}\left(1+\frac{M_1}{L_1}\tan\beta_2\tan\alpha\right)\right) \quad (4)$$

$$\dot{\beta}_2 = v\left(\frac{\tan\alpha}{L_1}-\frac{\sin\beta_2}{L_2}+\frac{M_1}{L_1L_2}\cos\beta_2\tan\alpha\right) \quad (5)$$

Call $\mathbf{p}=[y_3\ \theta_3\ \beta_3\ \beta_2]^T$ the configuration state obtained neglecting the longitudinal component x_3. In a compact way, the state equations are written as:

$$\dot{\mathbf{p}} = v\big(\mathcal{A}(\mathbf{p})+\mathcal{B}(\mathbf{p},\,\alpha)\big) \quad (6)$$

The sign of v decides the direction of motion, $v<0$ corresponding to backward motion. The entire state is measured via two potentiometers on the relative angles β_2 and β_3, and a pair of optical encoders on the two wheels of the rearmost axle.

A.1. State and input saturations. Both the relative angles β_2 and β_3 present hard constrains:

$$|\beta_2|\le\beta_{2_s}=0.6\text{ rad},\qquad |\beta_3|\le\beta_{3_s}=1.3\text{ rad} \quad (7)$$

These limitations are due to the front and rear body touching each other and to the dolly touching the wheels. They are particularly important since for back-up maneuvers the equilibrium point is unstable and jack-knife effects appear on both angles. The other two states do not present saturations, however for practical reasons of limited space when maneuvering, it is convenient to assume the following

$$|y_3|\le y_{3_s}=75\text{ cm}\qquad |\theta_3|\le\theta_{3_s}=\frac{\pi}{2}\text{ rad}$$

Summarizing, the domain of definition of $\mathbf{p}$ is

$$D=(-y_{3_s},\,y_{3_s})\times(-\theta_{3_s},\,\theta_{3_s})\times(-\beta_{3_s},\,\beta_{3_s})\times(-\beta_{2_s},\,\beta_{2_s}) \quad (8)$$

Also the input has a saturation:

$$|\alpha|\le\alpha_s=0.43\text{ rad} \quad (9)$$

The steering driver tolerates very quick variations, so we do not assume any slew rate limitation in the steering signal.

B. Jacobian linearization along trajectories

The system (6) is homogeneous in the longitudinal input v. Fixing v as a given nonnull function means having a drift component, which gives a nonvanishing term to the differential equations of the system. The steering angle

α can be used to give asymptotic stability to the system along a trajectory. The trajectories which admit a constant equilibrium point in this way are those corresponding to straight lines or arcs of circles. The first type of equilibrium involves 4 of the 5 states of (1)-(5), for example the vector $\mathbf{p}$, while for the circular trajectories only the relative posture $\bar{\mathbf{p}} = [\beta_3,\ \beta_2]^T$ has a constant equilibrium point in the system (6) (or a different basis, like that corresponding to a Frenet frame must be chosen, see [5], [27] for details).

B.1. Straight line linearization. The equilibrium point of $\mathbf{p}$ is the origin $\mathbf{p}_e = 0$ and it corresponds to a nominal value of the steering input $\alpha_e = 0$. The linearized system is

$$\dot{\mathbf{p}} = v\,(A\mathbf{p} + B\alpha) \tag{10}$$

where

$$A = \begin{bmatrix} 0 & 1 & 0 & 0 \\ 0 & 0 & \frac{1}{L_3} & 0 \\ 0 & 0 & -\frac{1}{L_3} & \frac{1}{L_2} \\ 0 & 0 & 0 & -\frac{1}{L_2} \end{bmatrix} \qquad B = \begin{bmatrix} 0 \\ 0 \\ -\frac{M_1}{L_1 L_2} \\ \frac{L_2+M_1}{L_1 L_2} \end{bmatrix} \tag{11}$$

B.2. Linearization along a circular trajectory. Consider the subsystem of (6) relative to $\bar{\mathbf{p}}$:

$$\dot{\bar{\mathbf{p}}} = v\big(\bar{A}(\bar{\mathbf{p}}) + \bar{B}(\bar{\mathbf{p}},\,\alpha)\big) \tag{12}$$

Proposition 1: The equilibrium point of (12) corresponding to a given steering angle α_e is:

$$\beta_{2_e} = \arctan\left(M_1/r_1\right) + \arctan\left(L_2/r_2\right) \tag{13}$$

$$\beta_{3_e} = \arctan\left(r_3/L_3\right) \tag{14}$$

where $r_1 = \frac{L_1}{\tan\alpha_e}$, $r_2 = \sqrt{r_1^2 + M_1^2 - L_2^2}$ and $r_3 = \sqrt{r_2^2 - L_3^2}$ are the radii of the circular trajectories followed by the midpoints P_1, P_2 and P_3 of the axles (see Fig.3).

Proof: At steady state, with nominal steering angle α_e, all the axles follow concentric circular trajectories. Look at Figure 3. All the calculations are straightforward

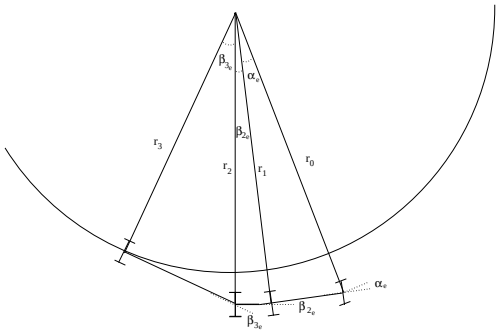

Fig. 3. Equilibrium point along an arc of circle.

from trigonometry, starting from a fixed α_e. ■

The linearization of (12) around $\bar{\mathbf{p}}_e = [\beta_{3_e}\ \beta_{2_e}]^T$ and α_e is now given by

$$\dot{\tilde{\mathbf{p}}} = v\big(\bar{A}(\bar{\mathbf{p}} - \bar{\mathbf{p}}_e) + \bar{B}(\alpha - \alpha_e)\big) \tag{15}$$

where

$$\bar{A} = \begin{bmatrix} \frac{\cos\beta_{2_e}\cos\beta_{3_e}}{L_3} & \frac{\cos\beta_{2_e}}{L_2} + \frac{\sin\beta_{2_e}\sin\beta_{3_e}}{L_3} + \frac{M_1}{L_1}\bar{f}(\bar{\mathbf{p}}_e)\tan\alpha_e \\ 0 & -\frac{\cos\beta_{2_e}}{L_2}\left(1 + \frac{M_1}{L_1}\tan\beta_{2_e}\tan\alpha_e\right) \end{bmatrix}$$

$\bar{f}(\bar{\mathbf{p}}_e) = \frac{\sin\beta_{2_e}}{L_2} - \frac{\cos\beta_{2_e}\sin\beta_{3_e}}{L_3}$ and

$$\bar{B} = \begin{bmatrix} -\frac{M_1}{L_1}\left(\frac{\cos\beta_{2_e}}{L_2} + \frac{\sin\beta_{2_e}\sin\beta_{3_e}}{L_3}\right)\left(1+\tan^2\alpha_e\right) \\ \frac{1}{L_1}\left(1 + \frac{M_1}{L_2}\cos\beta_{2_e}\right)\left(1+\tan^2\alpha_e\right) \end{bmatrix}$$

III. Local controllers for backward and forward motion

In this Section, we describe the local controllers to be used in the different regimes of motion: drive forward or backward and linearize along a straight line or an arc of circle.

A. Reversing along a line for the Jacobian linearization

Assume v is a given negative constant.

A.1. The linear quadratic controller. Consider the straight line backing case. The linearization (10) is open-loop unstable: the characteristic polynomial of the uncontrolled system is

$$\det\left(sI - vA\right) = s^2\left(s + \frac{v}{L_2}\right)\left(s + \frac{v}{L_3}\right) \tag{16}$$

Since (10) is controllable, the origin of the nonlinear system (6) can be made an asymptotically stable equilibrium by linear state feedback. We treat it as a linear quadratic optimization problem and in the weight assignment we use the rule of thumb of trying to have decreasing closed-loop bandwidths when moving from the inner loop to the outer one in a nested loopshaping design. In fact, the relative displacement y_3 comes after a cascade of two integrators from the relative angles as can be seen on the linearization (11). It turns out that such a heuristic reasoning is very important in the practical implementation in order to deal with the saturations.

Calling $K_B = BP_B$ the gain proposed by the solution of the LQ problem, where P_B is the solution of the Lyapunov equation, the closed loop linear system $\dot{\mathbf{p}} = v\,(A - BK_B)\,\mathbf{p}$ has two real and two complex conjugated eigenvalues; all three real parts are distinct. This is enough to say that the unconstrained linear closed-loop system forms a contraction map for positive times, $\max_{t\geq 0}\|e^{(A-BK_B)t}\| = 1$, where $\|\cdot\|$ is the operator norm. In other words, the ellipsoids of initial conditions containing the origin are positively invariant sets [2] for the closed loop linear system. Such ellipsoids are level surfaces of the quadratic Lyapunov function $V_B = \mathbf{p}^T P_B \mathbf{p}$.

A.2. Qualitative analysis of the basin of attraction. It is in general difficult to draw conclusions on the invariance properties of the flow of a nonlinear system. If in addition one takes into account the state and input constraints

(7)-(9), then an analytic description becomes almost impossible [10]. Therefore, in order to obtain estimates of the region of attraction of the linear controller $\alpha = -K_B\mathbf{p}$ and of the contractivity of the resulting integral curves, we rely on the numerical simulation of the closed-loop behavior of the original nonlinear system (6), paired with the linear controllerK_B:

$$\dot{\mathbf{p}} = \mathcal{F}_B(\mathbf{p}) = v\big(\mathcal{A}(\mathbf{p}) + \mathcal{B}(\mathbf{p},\, -K_B\mathbf{p})\big) \tag{17}$$

In order to obtain a graphical representation of the results, in the following we neglect the y_3 component of the state space, which is by far the less critical one with the LQ controller in use.

The cloud of initial conditions that represents the region of attraction closely resembles an ellipsoid in $\hat{\mathbf{p}} = [\theta_3\ \beta_3\ \beta_2]^T$ space. The fitting of an ellipsoid $\hat{\mathcal{E}}$ strictly contained in the set of succesfull initial conditions can be done by direct investigation, see Figure 4 (left). The principal axes $\hat{\mathbf{q}} = [q_1\ q_2\ q_3]^T$ of the ellipsoid are related to $\hat{\mathbf{p}}$ by an orthogonal transformation:

$$\hat{\mathbf{p}} = \hat{R}_{\mathcal{E}}\hat{\mathbf{q}} \qquad \hat{R}_{\mathcal{E}} \in SO(3)$$

Calling ε_1, ε_2 and ε_3 the semiaxes of $\hat{\mathcal{E}}$, the ellipsoid is given by the algebraic equation

$$\hat{\mathcal{E}} = \left\{ \frac{q_1^2}{\varepsilon_1^2} + \frac{q_2^2}{\varepsilon_2^2} + \frac{q_3^2}{\varepsilon_3^2} = 1 \right\} \tag{18}$$

Taking into account also the y_3 component of the initial conditions, the ellipsoid $\mathcal{E} \in \mathbb{R}^4$ is given by

$$\mathcal{E} = \left\{ \frac{q_1^2}{\varepsilon_1^2} + \frac{q_2^2}{\varepsilon_2^2} + \frac{q_3^2}{\varepsilon_3^2} + \frac{q_4^2}{\varepsilon_4^2} = 1 \right\} \tag{19}$$

with $\varepsilon_4 \gg \varepsilon_i,\ i = 1,\, 2,\, 3$. In D the difference with respect to Figure 4 (left) can hardly be appreciated.

From Figure 4 (left), we draw the qualitative conclusion that for the closed-loop nonlinear system $\hat{\mathcal{E}}$ is a positively invariant set.

B. Stabilization for forward motion

When $v > 0$, in (16) the two unstable poles move on the open left half of the complex plane. Considering the subsystem $\hat{\mathbf{p}}$ means neglecting one of the two poles in the origin. The origin of $\hat{\mathbf{p}}$ is asymptotically stabilizable by linear feedback and this time convergence for the nonlinear system in $\left(-\frac{\pi}{2},\, \frac{\pi}{2}\right) \times (-1.3,\, 1.3) \times (-0.6,\, 0.6)$ is a less critical problem. The reason for neglecting y_3 when moving forward is again the same: the closed loop mode relative to y_3 has a natural time constant higher of several orders of magnitude when compared to the other states.

Assume for example $v = 1$. Extracting from (11) the three dimensional system $(\hat{A},\, \hat{B})$, linearization around the origin of (3)-(5), it is possible to choose a gain $\hat{K}_F$ such that the closed loop system $\dot{\hat{\mathbf{p}}} = v(\hat{A} - \hat{B}\hat{K}_F)\hat{\mathbf{p}}$ is asymptotically stable and has three distinct real modes. The practical rule here for the selection of the eigenvalues is to try to have all 3 closed-loop poles of the same order of magnitude. The unavoidable input saturation will not destroy stability anyway. Assuming no control on y_3, the variation in y_3 due to the forward closed-loop is hard to compute explicitly, but a worst case analysis can give an upper bound on it.

Proposition 2: Assume the task of the forward controller $\hat{K}_F$ is to steer the system $(\hat{A},\, \hat{B})$ inside the ellipsoid $\mathcal{E}_\rho$. The variation on y_3 starting from any admissible initial condition $\mathbf{p}_0 = [y_{3_0}\ \theta_{3_0}\ \beta_{3_0}\ \beta_{2_0}]^T$ is bounded by

$$|\Delta y_3| \leq \frac{\mu\left|\cos\theta_{3_\rho} - \cos\theta_{3_0}\right|}{\left|\theta_{3_0}\lambda_{\min}(\hat{A} - \hat{B}\hat{K}_F)\right|} \tag{20}$$

with $\mu = \left|1 + \frac{M_1}{L_1}\tan\beta_{2_s}\tan\alpha_s\right|$ and $\theta_{3_\rho} = \sqrt{\rho\hat{\varepsilon}_{\max}}$.

Proof: From (2), if $\mu = \left|1 + \frac{M_1}{L_1}\tan\beta_{2_s}\tan\alpha_s\right|$ then

$$|\dot{y}_3| \leq \mu\,|\sin\theta_3(t)| \tag{21}$$

We need a bound on the value of $\theta_3(t)$ and to quantify the settling time t_s of the θ_3 mode from θ_{3_0} to its entering into the ellipsoid $\mathcal{E}_\rho$. Since for the forward motion stability is not a problem not even in presence of saturations, deriving a bound on the settling time of θ_3 we consider only the linearized system. The stable closed loop system $\dot{\hat{\mathbf{p}}} = (\hat{A} - \hat{B}\hat{K}_F)\hat{\mathbf{p}}$ has three distinct real modes. Its integral curves $\hat{\mathbf{p}}(t) = e^{(\hat{A} - \hat{B}\hat{K}_F)t}\hat{\mathbf{p}}_0$ can be bounded as follows:

$$\|e^{-|\lambda_{\max}(\hat{A} - \hat{B}\hat{K}_F)|I_3 t}\hat{\mathbf{p}}_0\|_2 \leq \|\hat{\mathbf{p}}(t)\|_2 \leq \|e^{-|\lambda_{\min}(\hat{A} - \hat{B}\hat{K}_F)|I_3 t}\hat{\mathbf{p}}_0\|_2$$

with I_3 the 3-dimensional identity matrix. Since there are no multiple closed loop eigenvalues, also the θ_3 mode alone is bounded by the slowest mode of the closed loop

$$|\theta_3(t)| \leq \left|e^{-|\lambda_{\min}(\hat{A} - \hat{B}\hat{K}_F)|t}\theta_{3_0}\right|$$

In order to compute t_s, we need to have a value of $\theta_3(t)$ which is certainly inside the ellipsoid $\hat{\mathcal{E}}_\rho :\ \left\{\hat{\mathbf{p}}^T\hat{P}_{\mathcal{E}}\hat{\mathbf{p}} = \rho\right\}$. The circle $\lambda_{\min}\left(\hat{P}_{\mathcal{E}}\right)\|\hat{\mathbf{p}}\|_2^2 = \min_{i=1,\,2,\,3}(\nu_i)\|\hat{\mathbf{p}}\|_2^2 = \rho$ (do not count ν_4) is contained inside $\hat{\mathcal{E}}_\rho$, therefore calling $\hat{\nu}_{\min} = \min_{i=1,\,2,\,3}(\nu_i) = \frac{1}{\max_{i=1,\,2,\,3}(\varepsilon_i)} = \frac{1}{\hat{\varepsilon}_{\max}}$, for the θ_3 variable alone $\theta_{3_\rho} = \sqrt{\rho/\hat{\nu}_{\min}} = \sqrt{\rho\hat{\varepsilon}_{\max}}$ does the job. The desired bound on the settling time is then

$$t_s = \frac{\left|\ln\frac{\theta_{3_\rho}}{\left|\theta_{3_0}\right|}\right|}{\left|\lambda_{\min}\left(\hat{A} - \hat{B}\hat{K}_F\right)\right|} \tag{22}$$

Integrating (21) from 0 to t_s:

$$|y_3(t) - y_{3_0}| \leq \mu\int_0^t \left|\sin\left(e^{-|\lambda_{\min}(\hat{A} - \hat{B}\hat{K}_F)|\tau}\theta_{3_0}\right)\right| d\tau$$

i.e.

$$\begin{aligned} |\Delta y_3| &\leq \frac{\mu\left|\cos\left(e^{-|\lambda_{\min}(\hat{A} - \hat{B}\hat{K}_F)|\tau}\theta_{3_0}\right) - \cos\theta_{3_0}\right|}{\left|\theta_{3_0}\lambda_{\min}(\hat{A} - \hat{B}\hat{K}_F)\right|} \\ &\leq \frac{\mu\left|\cos\theta_{3_\rho} - \cos\theta_{3_0}\right|}{\left|\theta_{3_0}\lambda_{\min}(\hat{A} - \hat{B}\hat{K}_F)\right|} \end{aligned}$$

■

Since t_s is inversely proportional to the smallest eigenvalue of the closed loop, the more the slowest mode (i.e. θ_3) is "speeded up" by $\hat{K}_F$ the sooner $\hat{\mathbf{p}}$ enters inside $\mathcal{E}_\rho$. Obviously, moving eigenvalues deeper in the left half of the complex plane implies more problems with the input saturation.

The bound (20) can be used to characterize the region of attraction in D for an ellipsoid like $\hat{\mathcal{E}}_\rho$ as attractor set for the forward motion case. Neglecting the input saturation, it basically coincides with D except for a cut in the y_3 direction.

Corollary 1: In D, the region of attraction to an ellipsoid $\hat{\mathcal{E}}_\rho$ of the controller $\hat{K}_F$ is given by

$$D_\rho = (-y_{3_s} + \Delta y_{3_s},\ y_{3_s} - \Delta y_{3_s}) \times (-\theta_{3_s},\ \theta_{3_s}) \times \times (-\beta_{3_s},\ \beta_{3_s}) \times (-\beta_{2_s},\ \beta_{2_s}) \quad (23)$$

where $\Delta y_{3_s}(\rho) = \frac{\left|1+\frac{M_1}{L_1}\tan\beta_{2_s}\tan\alpha_s\right| \left|\cos\theta_{3_\rho} - \cos\theta_{3_s}\right|}{\left|\theta_{3_s}\,\lambda_{\min}(\hat{A}-\hat{B}\hat{K}_F)\right|}$.
Such a restriction is not really drastic; in numbers, with our choice of $\hat{K}_F$, it amounts to about 30 cm. Furthermore, one can add that Δy_{3_s} is a worst case bound and that the choice of $y_{3_s} = 75$ cm is purely arbitrary.

C. Reversing along an arc of circle (alignment control)

If instead of $\mathbf{p}$ or $\hat{\mathbf{p}}$ only the backward stabilization of the relative angles $\bar{\mathbf{p}} = [\beta_3\ \beta_2]$ is required, then a linearization like (15) can be used and the desired equilibrium point $\bar{\mathbf{p}}_e$ can be indifferently the origin or a pair of constant angles like in (13)-(14). In this case, the truck and trailer will be stabilized along a circular trajectory as computed in Proposition 1. We can consider the circular trajectories corresponding to e.g. $|\alpha_e| \le \alpha_{e_s} = \frac{4}{5}\alpha_s$ (see Proposition 1 for the corresponding radii), for which the equilibrium point is compatible with the system constraints and a certain margin is left around it before reaching the steering actuator saturation. The controller $\alpha = -\bar{K}_B\bar{\mathbf{p}}$ can be computed like in Section III-A by another LQ problem. The region of attraction of the equilibrium is an ellipse in the $\bar{\mathbf{p}}$ plane, for each value of α_e in $|\alpha_e| \le \alpha_{e_s}$. If a Frenet frame is chosen on the arc of circle [27], then the encoders information can be used to attain local stabilization of $\mathbf{p}$ (and not just of $\bar{\mathbf{p}}$) along the desired arc.

IV. Switching controller

The region of attraction of the backward controller is only a subset $\hat{\mathcal{E}}$ of the entire domain D. Starting from outside $\hat{\mathcal{E}}$, it is necessary to first drive forward for example with a controller like $\hat{K}_F$ until the system enters inside $\hat{\mathcal{E}}$ and only then switch to backward motion. When reversing, the main manifestation of a destabilizing perturbation is a jack-knife effect on the relative angles. Just like on a full-scale truck and trailer vehicle, the only way to recover from such a situation is to move forward and try again. So, in order to guarantee stability of the backward motion in D and not only inside the ellipsoid $\hat{\mathcal{E}}$ for the nominal model and in order to cope with the perturbations, one single controller is not enough. The switching variable between the two controllers is the longitudinal velocity v. For example we assume that $v \in \{-1, +1\} \triangleq \mathcal{I}$. The backward regime is selected by $v = -1$ and the forward one by $v = +1$. Since the longitudinal input v is a control input, if we assume that $v \in \mathcal{I}$ then v becomes a controlled logic variable. Moreover, if the selection of the logic value of v is made according to a partition of the state space, the overall system with multiple controllers becomes a feedback controlled system. This is feasible in our case since we have on-line full state information available.

A. Selection of the two switching surfaces

Two are the switching surfaces that delimit the partition of the state space, and their crossing in a prescribed direction by the flow of the system induces a sign change in v. This, in its turn, causes the inversion of the direction of motion and induces the activation of the corresponding linear state feedback controller. These switching surfaces, call them $\mathcal{S}_{-+}$ and $\mathcal{S}_{+-}$ have to be chosen such that they give to the point $\mathbf{p} = 0$ of the backward motion the character of global attractor (in D). Since in both regimes the origin is the closed-loop local asymptotically stable equilibrium point, we choose both $\mathcal{S}_{-+}$ and $\mathcal{S}_{+-}$ as closed hypersurfaces in $\mathbb{R}^4$ containing the origin in their interior.

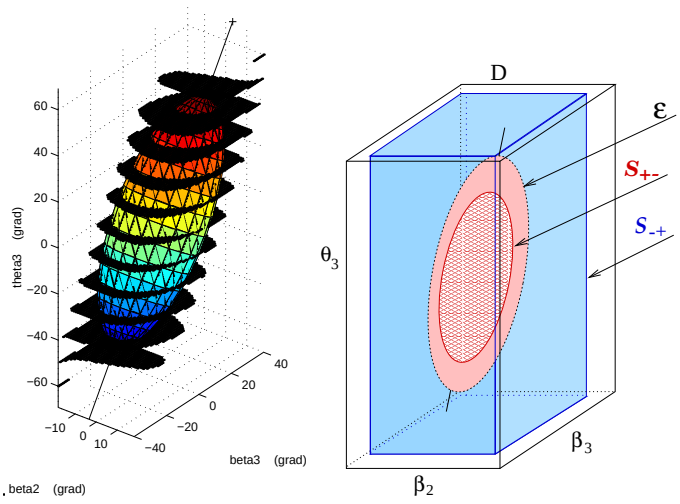

Fig. 4. Left: the succesful initial conditions and the fitted ellipsoid $\hat{\mathcal{E}}$. Right: the switching surfaces (in $\mathbb{R}^3$).

The switching surface from forward to backward motion: $\mathcal{S}_{+-}$. From Section III-A, $\mathcal{S}_{+-}$ has to be contained inside $\mathcal{E}$. The simplest choice is to consider $\mathcal{S}_{+-} = \mathcal{E}_\rho$ for some ρ such that $\frac{1}{2} < \rho < 1$. The trade-off is the following:

- if $\mathcal{S}_{+-}$ is large ($\rho \to 1$) the system will be sensitive to disturbances and more easily destabilized by perturbations (meaning more switches can occur);
- if $\mathcal{S}_{+-}$ is small ($\rho \to \frac{1}{2}$) the forward regime will be very long, which is often unacceptable for practical implementations.

Ellipsoids smaller that $\mathcal{E}_{\frac{1}{2}}$ are also not recommendable for other reasons, like the possibility of being completely "jumped over" in case of relevant sensor error.

A.1. The switching surface from backward to forward motion: $\mathcal{S}_{-+}$. Such a switching surface has to "tell" the system that backing is not going well and the trailers need to be realigned. The choice is quite flexible, the only constraint is that $\mathcal{S}_{+-}$, $\mathcal{S}_{-+}$ and the sides of D must not intersect. In particular the set distance between $\mathcal{S}_{+-}$ and $\mathcal{S}_{-+}$ gives the hysteresis between the two regimes. If this distance is positive, problems like chattering will be avoided. One simple choice for $\mathcal{S}_{-+}$ is for example to use a cube in $\mathbb{R}^4$ which is a rescaling of D by a factor less than 1.

B. Control logic for v

D is divided into three nonintersecting regions:
- $\mathcal{C}_-$ = region inside $\mathcal{S}_{+-}$ where $v = -1$;
- $\mathcal{C}$ = region between $\mathcal{S}_{-+}$ and $\mathcal{S}_{+-}$ where v can be either $+1$ or -1;
- $\mathcal{C}_+$ = region outside $\mathcal{S}_{-+}$ ($\mathcal{C}_+ = D \cap (\mathcal{C} \cup \mathcal{C}_-)^{\perp}$) where $v = +1$.

Changes on v occur only at crossing with the rules of the finite state machine of Figure 5.

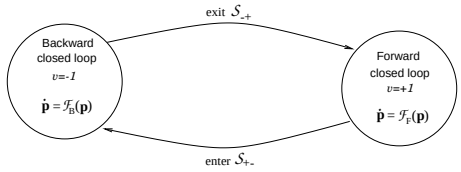

Fig. 5. The hybrid automaton associated with the control logic.

C. Convergence for the nominal and perturbed system

For the nominal system we can assert the following:

Theorem 1: Under the assumptions of invariance of $\mathcal{E}$, the system (6) with the two controllers $\hat{K}_F$ and K_B , respectively for the cases $v = -1$ and $v = +1$, and with the feedback rule of Figure 5 for $v \in \mathcal{I}$, asymptotically coverges to the origin in backward motion from any inital condition in D_ρ.

Proof: From the analysis of Section III and looking at the switching rules of Fig. 5, the following order relation is the only possible one for the system:

$$\underset{v=+1}{\mathcal{C}_+} \quad \rightarrow \quad \underset{v=+1}{\mathcal{C}} \quad \rightarrow \quad \underset{v=-1}{\mathcal{C}_-}$$

In fact, from any $\mathbf{p}_0 \in D_\rho$, the controller K_B steers the system inside $\mathcal{S}_{+-}$ and $\mathcal{S}_{+-}$ is a positively invariant set for the controller $\hat{K}_F$. In the two regions $\mathcal{C}_+$ and $\mathcal{C}$ the controller K_B stabilizes only $\hat{\mathbf{p}}$. Once $\mathcal{S}_{+-}$ is fixed so is D_ρ, and in D_ρ the corresponding excursion on y_3 cannot exit D by Corollary 1. ■

So for the nominal system the switching surface $\mathcal{S}_{-+}$ is never in use. Due to the unstable equilibrium point, the effect of perturbations is critical in $\mathcal{C}_-$. Since the whole stabilization developed here occurs along a trajectory, we cannot expect the perturbations affecting the system to be vanishing at the equilibrium point of (17). For example, the two potentiometers for the measure of the relative angles β_2 and β_3 introduce an error of $\pm 4^\circ$ also at steady state. Similarly, all the disturbances affecting the real system can be considered nonvanishing. When a perturbation is large enough to pull the state out of $\mathcal{E}$ the system diverges. Trying to quantify the amplitude of the destabilizing pertubations and, consequently, trying to inferr total stability for a class of bounded perturbations is very hard in our situation because of the input saturation involved. The destabilized system keeps driving backwards until it hits the $\mathcal{S}_{-+}$ surface. After that, it inverts the direction of motion and tries again to converge inside $\mathcal{S}_{+-}$ with the forward controller. In this part, stability is not undermined by the pertubations because the system is open-loop stable, but perhaps the convergence rate (and therefore the settling time t_s and Δy_3) can be.

As said above, if the $\mathcal{S}_{-+}$ and $\mathcal{S}_{+-}$ do not touch each other, degenerate switching phenomena (normally referred to as Zeno chattering) do not occur. Furthermore, also the different pole placement philosophy adopted in the two controllers $\hat{K}_F$ and K_B (in one the critical mode, the θ_3 mode, is slow, in the other it is instead faster) is meant to avoid a chattering type of behavior (like keep moving the system back and forth between the same points on $\mathcal{S}_{-+}$ and $\mathcal{S}_{+-}$) which can happen if the two closed-loops resemble each other.

V. Another switching scheme

At the switching $\mathcal{C} \xrightarrow{\mathcal{S}_{+-}} \mathcal{C}_-$, if $|\theta_3|$ is large, instead of the controller $\hat{K}_F$ one can think of using a different strategy, based on realigning only the β_2 and β_3 angles leaving θ_3 free, and then recover θ_3 if needed by reversing along an arc of circle with $\bar{K}_B$. Neglecting θ_3 in the forward motion means reducing considerably its duration, as the θ_3 mode is the slowest of the three. This strategy allows to greatly increase the convergence rate when y_3 is large and $y_3 \cdot \theta_3 > 0$. A typical situation is shown in Figure 6. The modes needed for its implementation are three:

1. forward control of β_2 and β_3;
2. reverse along arc of circle;
3. reverse along straight line.

Assume $v = -1$, $\theta_3 > 0$ and $y_3 > 0$ (Figure 6). Call $\tilde{\mathbf{p}}$

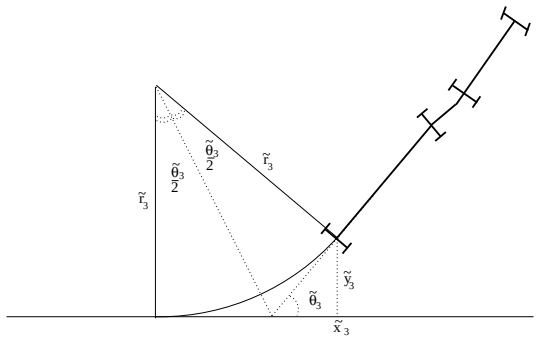

Fig. 6. Calculation of the arc of circle for reverse motion.

the state on the switching surface $\bar{\mathcal{S}}_{+-}$ and $\tilde{x}_3$ the corresponding coordinate on the reference line. The arc of circle tangent to both the line through the point $(x_3,\, y_3)$ of orientation $\tilde{\theta}_3$ and to the straight line $y_3 = 0$ is unique it has radius $\tilde{r}_3 = \frac{\bar{y}_3}{\sin\bar{\theta}_3 \tan\frac{\bar{\theta}_3}{2}}$ and center of rotation $\left(\tilde{x}_3 - \frac{\bar{y}_3\left(1+\cos\bar{\theta}_3\right)}{\sin\bar{\theta}_3},\ \frac{\bar{y}_3}{\sin\bar{\theta}_3\tan\frac{\bar{\theta}_3}{2}}\right)$. Since $v = -1$, we take the length of the arc from P_3 to the axis $y_3 = 0$, $\tilde{r}_3 \cdot \tilde{\theta}_3$, as duration of the reversing along arc of circle mode i.e. as time between the switch $v : +1 \rightarrow -1$ and the switch from reversing along arc of circle to reversing along straight line. The $\mathcal{S}_{-+}$ switching surface remains in use while for the switching $v : +1 \rightarrow -1$ we consider only the β_2, β_3 angles: $\bar{\mathcal{S}}_{+-} = \left\{\beta_2^2/\bar{\varepsilon}_2^2 + \beta_3^2/\bar{\varepsilon}_3^2 = 1\right\}$ with $\bar{\varepsilon}_2$ and $\bar{\varepsilon}_3$ of the same order of magnitude. The forward controller then is a reduced version of $\hat{K}_F$ with only two nonnull gains. The reduced system (12) with $v = +1$, $\bar{\mathbf{p}}_e = [0\ 0]^T$ is asymptotically stabilizable and the duration of the forward motion between $\mathcal{S}_{-+}$ and $\bar{\mathcal{S}}_{+-}$ is normally quite short compared to that of Section IV. Calling $\tilde{t}$ the time at which the flow of the system hits $\bar{\mathcal{S}}_{+-}$, the complete hybrid automaton is depicted in Figure 7.

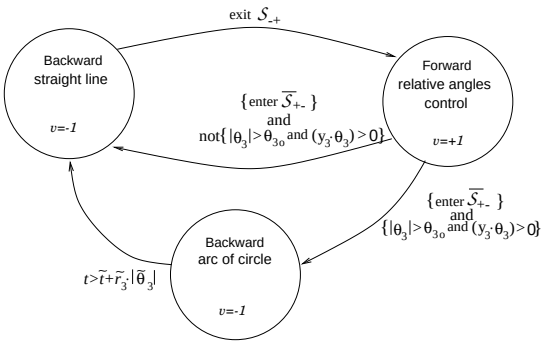

Fig. 7. The new hybrid automaton.

VI. Practical implementation and experimental results

For the truck and trailer shown in Figure 1, the controller was implemented using a commercial version of PC/104. It was written in C-language and used at a frequency of about 10Hz since the velocity of the system was very low. Fig. 8-9 present the result of a simple real maneuver. The switching scheme used is the two-state automaton described in Section IV. The vehicle starts with saturated relative angles and first drives forward in order to realign itself, then reverses along the reference line. Notice that since the θ_3 mode is slower than those of the relative angles, most of the forward motion is needed to get θ_3 inside the ellipsoid $\mathcal{S}_{+-}$. It is instructive to compare (Figure 9, right) the activity of the feedback input when the open loop system is stable (upper plot) and when it is unstable (lower plot). The experimental validity of the heuristic ellipsoid $\mathcal{E}$ was verified by several trials. For the backward controller K_B alone, some of the unsucessful initial conditions belonging to the quadrant ($\theta_3 = 0$, $\beta_2 \leq 0$, $\beta_3 \leq 0$) are shown in

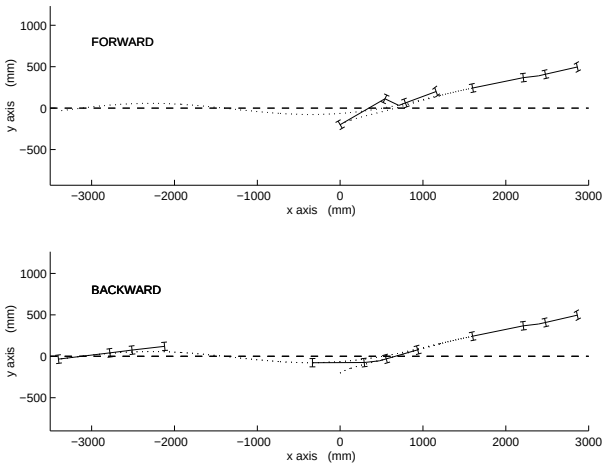

Fig. 8. Experiment # 1: sketch of the motion of the vehicle. The dotted line represents the path followed by the (x_3, y_3) point.

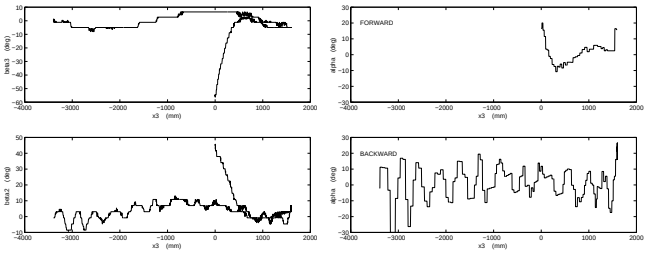

Fig. 9. Experiment # 1: relative angles β_3 and β_2 (left) and steering input α (right).

Fig. 10: they all lay outside $\mathcal{E}$. In the same picture the switched integral curve used in the experiment of Fig. 8 is also reported. In this experiment we use $\mathcal{S}_{+-} = \mathcal{E}_{4/5}$. As expected, after entering inside $\mathcal{E}$, the trajectory does not escape anymore. The second experiment (Fig. 11) shows part of the switching scheme described in Section V. Starting from a jack-knife position, the vehicle moves forward, realigns the relative angles and then reverses along an arc of circle until hitting the desired reference line. At this point the third state (reversing along the straight line) takes over (not shown in the experiment). Notice how the forward part of the motion is shorter than in the first experiment as only the two relative angles are considered in the realignment.

References

[1] B. Anderson and J.B Moore. *Optimal control. Linear quadratic methods*. Prentice Hall, 1989.

[2] F. Blanchini. Set invariance in control (Survey paper). *Automatica* **35**:1747-1767, 1999.

[3] P.Bolzern, R.M. De Santis, A Locatelli and D. Masiocchi. Path-tracking for articulated vehicles with off-axle hitching. *IEEE Transaction on Control Systems Technology*, **6**:515-523,1998.

[4] F. Bullo and R. Murray. Experimental comparison of trajectory trackers for a car with trailers. *IFAC World Congress*, San Francisco, CA, 1996.

[5] C. Canudas de Wit. Trends in mobile robot and vehicle control. In K.P. Valavanis and B. Siciliano (eds), Control problems in robotics. Lecture notes in control and information sciences, Springer-Verlag, 1998.

[6] K. Chellapilla. Evolving nonlinear controllers for backing up a

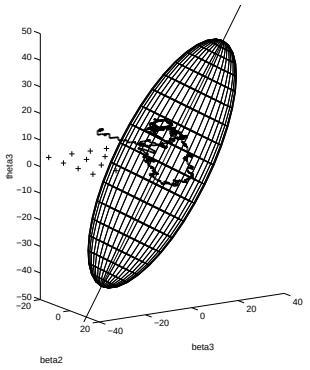

Fig. 10. The trajectory of Fig. 8 in the $\hat{\mathbf{p}}$ space and the ellipsoid $\hat{\mathcal{E}}$. The points + represent initial conditions from which the backwards controller alone fails to converge on experimental trials.

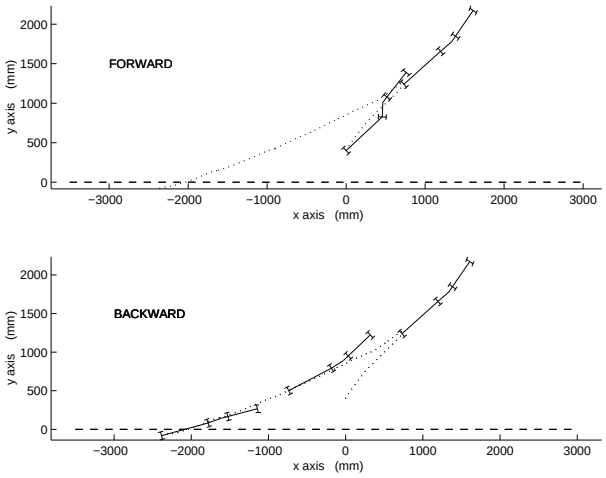

Fig. 11. Experiment # 2: sketch of the motion of the vehicle. The dotted line represents (x_3, y_3).

truck-and-trailer using evolutionary programming. Evolutionary Programming VII.7th International Conference, p.417-26, 1998.

[7] A.W. Divelbiss and J. Wen. Nonholonomic path planning with inequality constraints. Proc. 1994 IEEE Int. Conf. on Robotics and Automation, p.52-57.

[8] J De Dona. *Input Constrained linear control*. PhD thesis, Department of Electrical and Computer Engineering, The University of Newcastle, Australia. February 2000.

[9] M. Fliess, J. Levine, P. Martin and P. Rouchon. Flatness and defect of nonlinear systems: introductory theory and examples. *Int. Journal of Control*, **61**(6):1327-1361, 1995.

[10] E.G. Gilbert and K.T. Tan. Linear systems with state and control constraints: the theory and application of maximal output admissible set. *IEEE Transactions on Automatic Control*, **36**:1008-1020, 1991.

[11] S. K. Halgamuge, T.A. Runkler and M. Glesner. A hierarchical hybrid fuzzy controller for realtime reverse driving support of vehilces with long trailers. Proc. of the Third IEEE Conference on Fuzzy Systems.IEEE World Congress on Computational Intelligence p.1207-1210, 1994.

[12] D.F. Hougen, M. Gini and J. Slagle. Rapid unsupervised connectionist learning for backing a robot with two trailers. Proc. 1997 IEEE Int. Conf. on Robotics and Automation, p.2950-2955, Albuquerque, NM.

[13] R.E. Jenkins and B.P. Yuhas. A simplified neural network solution through problem decomposition: the case of the truck backer-upper. *IEEE Transactions on Neural Networks*, **4**:718-720, 1993.

[14] R. E. Kalman. When is a linear control system optimal? *Trans. of the ASME, Journal of Basic Engineering*, p.51-60, March 1964.

[15] D.H Kim and J.H Oh. Experiments of backward tracking control for trailer systems. Proc. 1999 IEEE Int. Conf. on Robotics and Automation, p.19-22, Detroit, MI.

[16] G.S. Kong and B. Kosko. Adaptive fuzzy systems for backing up a truck and trailer. *IEEE Trans. on Neural Networks*,**3**:211-223, 1992.

[17] J.R. Koza. A genetic approach to finding a controller to back up a tractor-trailer truck. Proc. of 1992 American Control Conference, p.2307-11,1992.

[18] F. Lamiraux and J.P. Laumond. A practical approach to feedback control for a mobile robot with trailer. Proc. 1998 IEEE Int. Conf. on Robotics and Automation, p.3291-3296, Leuven Belgium.

[19] J.P. Laumond (ed). Robot Motion Planning and Control, Lecture notes in control and information sciences, Springer-Verlag, 1998.

[20] W. Li, T. Tsubouchi and S. Yuta. On a manipulative difficulty of a mobile robot with multiple trailers for pushing and towing. Proc. 1999 IEEE Int. Conf. on Robotics and Automation, p.13-18, Detroit, MI.

[21] D. Liberzon and A. S. Morse. Basic problems in stability and design of switched systems. IEEE Control Systems Magazine, **19**:59-70,1999.

[22] W.H Ma and H Peng. Worst-case maneuvers for the roll-over and jackknife of articulated vehicles. Proc. of the American Control Conference, p.2263-2267, Philadelphia, PN, 1998.

[23] Y Nakamura, H. Ezaki, Y. Tan; W. Chung. Design of steering mechanism and control of nonholonomic trailer systems. Proc. 2000 IEEE Int. Conf. on Robotics and Automation, p.247 - 254, San Francisco, CA.

[24] M. van Nieuwstadt and R. Murray. Real time trajectory generation for differentially flat systems. *International Journal of Robust and Nonlinear Control*,**8**:995-1020,1998.

[25] D. Nguyen and B-Widrow. The truck backer-upper: an example of self-learning in neural networks. Proc. of SPIE vol.1293, pt.1,p.596-602, 1990.

[26] R. Parra-Loera and D.J. Corelis. Expert system controller for backing-up a truck-trailer system in a constrained space. Proc. of the 37th Midwest Symposium on Circuits and Systems p.1357-1361,1995.

[27] C. Samson. Control of chained systems: application to path-following and time-varying point stabilization of mobile robots. *IEEE Trans. on Automatic Control*, **40**,64-77, 1995.

[28] O. J. Sørdalen. Conversion of the kinematics of a car with n trailers into chained form. Proc. IEEE Int. Conf. on Robotics and Automation, p.382-387, Atlanta, Georgia, 1993.

[29] M. Sampei, T. Tamura, T. Kobayashi and N. Shibui. Arbitrary path tracking control of articulated vehicles using nonlinear control theory. *IEEE Transaction on Control Systems Technology*, **3**, 125-131, 1995.

[30] K. Tanaka, T. Taniguchi and H.O. Wang. Trajectory control of an articulated vehicle with triple trailers. Proc. 1999 IEEE International Conference on Control Applications, p.1673-8.

[31] D. Tilbury, R. Murray and S. Sastry. Trajectory generation for the N-trailer problem using Goursat normal form. *IEEE Trans. on Automatic Control*, **40**,802-819,1995.